



Molecular modelling of zinc sulphide nanoparticles stabilized by cetyltrimethylammonium bromide

PETR KOVÁŘ¹, PETR PRAUS^{2,3*}, MIROSLAV POSPÍŠIL¹ and RICHARD DVORSKÝ^{4,5}

¹Charles University in Prague, Faculty of Mathematics and Physics, Ke Karlovu 3, 12116 Prague 2, Czech Republic, ²Institute of Environmental Technology, VŠB-Technical University of Ostrava, 17. Listopadu 15, 708 33 Ostrava-Poruba, Czech Republic, ³Department of Chemistry, VŠB-Technical University of Ostrava, 17. Listopadu 15, 708 33 Ostrava-Poruba, Czech Republic, ⁴Institute of Physics, VŠB-Technical University of Ostrava, 17. Listopadu 15, 708 33 Ostrava-Poruba, Czech Republic and ⁵Regional Materials Science and Technology Centre, VŠB-Technical University of Ostrava, 17. Listopadu 15, 708 33 Ostrava-Poruba, Czech Republic

(Received 15 November 2013, revised 28 February 2014, accepted 10 May 2014)

Abstract: ZnS nanoparticles stabilized by cetyltrimethylammonium bromide (CTAB) were modelled in the Materials Studio environment. Four types of models with different distances between the ZnS nanoparticles and different amounts of cetyltrimethylammonium (CTA) cations without water and in a water environment were built and characterized by calculation of sublimation energies. The results of the molecular modelling without water showed that the most favourable model consisted of two ZnS nanoparticles with a distance of 8–9 nm separated without immersion of CTAs. On the contrary, the most favourable model in a water environment was composed of ZnS nanoparticles that nearly touched each other. CTA cations exhibited a tendency to be located on the ZnS surface forming sparse covers. The size distributions of the ZnS nanoparticles obtained by transmission electron microscopy (TEM) measurements agreed well with the molecular modelling results.

Keywords: molecular modelling; ZnS nanoparticles; cetyltrimethylammonium bromide; interactions.

INTRODUCTION

Semiconductor nanoparticles, such as metal oxides or metal sulphides, are well known for their outstanding electrochemical properties, which make them utilizable in photo-optics, opto-electronics, photocatalysis, etc.¹ One of the most important factors related to nanomaterials is the dependence of physical and chemical properties on their particle sizes. Decreasing particle size of a semicon-

*Corresponding author. E-mail: petr.praus@vsb.cz
doi: 10.2298/JSC131115050K

ductor leads to an increase of its specific surface area and gap energy, which is known as the quantum size effect or quantum confinement.^{2,3}

Zinc sulphide is a semiconductor with a wide direct band gap energy of about 3.7 eV. ZnS nanoparticles have been synthesized by precipitation of zinc ions with sulphides forming ZnS in the sphalerite (solubility product, $K_s = 1.6 \times 10^{-4}$) and wurtzite structure ($K_s = 2.5 \times 10^{-22}$). Freshly prepared ZnS nanoparticles, as well as other nanoparticles, tend to agglomerate and, therefore, are mostly stabilized by macromolecules or surfactants.^{4–6}

Stabilization mechanisms of nanoparticles cannot be directly observed by laboratory experimental methods but can be simulated by molecular modelling based on empirical force fields. The analysis of some the characteristics of the interaction energy can provide information on the stability of systems, mutual interactions of their parts and probability estimation for some processes.

The aim of this work was to model the interactions between ZnS nanoparticles and CTAB by molecular simulations. From the simulation point of view, some authors published papers dealing with structure of ZnS nanoparticles and their characteristics, *e.g.*, structural changes of the ZnS nanostructure depending on its size and on the species surrounding the nanoparticles.^{7–10} Although interactions between CTAB and some nanoparticles were modelled by several authors,^{11,12} mutual interactions of ZnS nanoparticles stabilized by CTAB were simulated for the first time in this study. In previous papers,^{4,5} only the structure of CTAB layers formed on the ZnS nanoparticles surface were modelled. Along with molecular modelling, colloid dispersions of ZnS nanoparticles and CTAB were examined by transmission electron microscopy, and the growth of the ZnS nanoparticles was studied to confirm the modelling results.

EXPERIMENTAL

Material and chemicals

The used chemicals were of analytical reagent grade: zinc acetate, sodium sulphide, (all from Lachema, Czech Republic), cetyltrimethylammonium bromide (Sigma, USA). Water deionised by reverse osmosis (Aqua Osmotic, Czech Republic) was used for the preparation of all solutions.

Precipitation of ZnS nanoparticles

ZnS nanoparticles were precipitated by adding zinc acetate to sodium sulphide.⁶ The precipitation was performed in the micellar dispersion of CTAB with the concentration of 3 mmol L⁻¹. The S²⁻:Zn²⁺ mole ratio was kept at 1.5:1.

Transmission electron microscopy

Transmission electron microscopy was performed on a JEM 1230 (Jeol, Japan) microscope operated at 80 kV. The freshly prepared samples of the ZnS nanoparticles stabilized by CTAB were placed on a copper grid (400 mesh) coated by a film of 1.5–3 % of poly(vinyl formaldehyde) in chloroform and dried by blotting paper. The contrast of the micrographs was improved by the addition of a 1 % solution of ammonium molybdate to the samples.

Molecular modelling

The data for the wurtzite structure were used for building the ZnS nanoparticles.⁶ Crystallographic data for wurtzite are the following: space group P6₃mc, $a = b = 0.382$ nm, $c = 0.626$ nm.¹³ According to experimental data, nanoclusters in the shape of a sphere with radii of 2.0 nm were created in a nanostructure builder module and two ZnS nanoparticles were used in the simulations. Molecular modelling was performed in the Materials Studio modelling environment.¹⁴

Since the CTAB molecule dissociates in water to form a CTA cation and a bromide anion, interactions of ZnS nanoparticles and CTA cations were modelled. The ZnS nanoparticle with adsorbed CTA cations was denoted as ZnS–CTA in this manuscript. The interactions and structure of two ZnS–CTA nanoparticles can be subsequently generalized for interactions and behaviour of a larger amount of ZnS–CTA ones. The number of CTA cations surrounding each ZnS nanoparticle was 30, 50, 70 and 90 and the following four models were built:

1. ZnS nanoparticles were nearly touching each other; the distance between ZnS nanoparticle centres was about 4.0 nm.
2. One ZnS–CTA nanoparticle shared CTA cations with other ZnS–CTA nanoparticle so that CTA cations were immersed in one another. The distance between the centres of the ZnS nanoparticles was about 6.0 nm.
3. ZnS–CTA nanoparticles were connected together *via* CTA chains. Models were used with various amounts of CTA (12–25), which formed chains of various distances between ZnS nanoparticle centres, ranging from 8.0 to 10.0 nm.
4. ZnS–CTA nanoparticles were separated without immersing CTA cations and without chain connection. The distance between ZnS centres ranged from 8.0 to 9.0 nm.

For each type of presented structure model, a set of initial models was created and the models were optimized without water and in a water environment. The models optimized without water contained two ZnS nanoparticles and CTA cations. Each model optimized in a water environment contained an additional 5760 water molecules together with compensating bromide anions randomly surrounding the ZnS nanoparticles. As found recently,^{4,5} the ZnS–CTA structure exhibited a bilayer arrangement of CTA cations around the ZnS nanoparticles, *i.e.*, half of CTA cations were oriented with their polar headgroup towards the outer space and the half with their polar headgroup towards the ZnS nanoparticle surface. In case of model 1, due to the close arrangement of ZnS nanoparticles, some of the CTA exhibited a bilayer arrangement and some was randomly distributed around the ZnS nanoparticles and among the CTA cations in the bilayer arrangement. The geometry optimization was realised in the Universal force field¹⁵ in the Materials Studio modelling environment. The advantage of this force field is a high speed of convergence, especially in case of large systems like those presented in this paper. On the other hand, the parameters in this force field can be used for a wide class of structure, which leads to less precise results, *e.g.*, infrared spectra. Nevertheless, this force field was employed in previous papers^{4,5} dealing with one ZnS–CTA nanoparticle and the results were in a good agreement with the experimental data. Therefore, this force field was used for the simulation of two ZnS–CTA particles. The geometry optimization was performed with all variable atomic positions and with the following convergence criteria: $E = 1 \times 10^{-4}$ kcal mol⁻¹*, force = 0.05 kcal mol⁻¹ nm⁻¹ and atomic displacement of 5×10^{-6} nm. The electrostatic and van der Waals energy were calculated by cubic spline with a cut-off distance of 1.55 nm. The charges of ZnS nanoparticles were calculated by the QEq method (charge equilibrium

* 1 kcal = 4.184 kJ

approach)¹⁶ and the partial charges of water molecules and CTA cations were assigned by the Compass force field.¹⁷

After geometry optimization, the models with the lowest energy were chosen for quench dynamics. The quench molecular dynamics simulations were performed in an NVT statistical ensemble (constant number of particles, constant volume and constant temperature) at a temperature of 298 K. One step of the simulation was 0.5 fs and 500–1000 ps were performed. The time interval between two quenches was 50000 steps (25 ps) of the simulation. The atomic positions of the ZnS nanoparticles were fixed and the other atomic positions were variable during the simulations. After quench dynamics, the optimized models with minimum energy were selected and they were subsequently minimized with the requested convergence criteria mentioned above and with all atomic positions variable to obtain the final structure of the models.

RESULTS AND DISCUSSION

Models of ZnS nanoparticles without water

Although real ZnS nanoparticles were dispersed in water, mutual interactions of two ZnS–CTA nanoparticles without water were calculated for comparison and the results are summarized in Table I. This table shows the dependence of the total sublimation energy E_{total} , which is the sum of van der Waals E_{vdw} and electrostatic E_{elst} interaction energies between ZnS–CTA nanoparticles, on the number of CTA cations for all the tested models. The interactions were calculated as interactions between rigid bodies. A rigid body is defined as a part

TABLE I. Total sublimation energies for various types of models and CTA concentrations without water

| No. of CTA cations | $E_{\text{total}} / \text{kcal mol}^{-1}$ | $E_{\text{vdw}} / \text{kcal mol}^{-1}$ | $E_{\text{elst}} / \text{kcal mol}^{-1}$ |
|--------------------|---|---|--|
| Model 1 | | | |
| 30 | -81 | -8 | -73 |
| 50 | -59 | -10 | -49 |
| 70 | -37 | -13 | -24 |
| 90 | -27 | -16 | -11 |
| Model 2 | | | |
| 30 | -96 | -10 | -86 |
| 50 | -74 | -11 | -63 |
| 70 | -37 | -1 | -36 |
| 90 | -40 | -15 | -25 |
| Model 3 | | | |
| 30 | -94 | -8 | -86 |
| 50 | -70 | -9 | -61 |
| 70 | -54 | -11 | -43 |
| 90 | -41 | -14 | -27 |
| Model 4 | | | |
| 30 | -99 | -10 | -89 |
| 50 | -79 | -10 | -69 |
| 70 | -58 | -13 | -45 |
| 90 | -45 | -14 | -31 |

of a system where all the interactions (bonded and non-bonded) between atoms within this part are neglected. To investigate the stability and probability of the occurrence of various models, the total sublimation energy (Table I) was divided into several energy contributions: *i*) interactions between CTA cations and ZnS nanoparticles, *ii*) interactions between CTA cations and *iii*) interactions between ZnS nanoparticles.

The interactions between CTAs and ZnS nanoparticles were the main energy contribution to the E_{total} sublimation energy. The average CTA and ZnS interactions of all amounts of CTA for models 1 and 3 exhibited higher energy values ($-64 \text{ kcal mol}^{-1}$) than for models 2 and 4 ($-71 \text{ kcal mol}^{-1}$). This could be explained by the fact that in models 2 and 4, all the CTA cations interacted with the ZnS nanoparticle surface *via* attractive interactions while some of the CTA cations in models 1 and 3 interacted only with one another *via* repulsive interactions. Moreover, the CTA–ZnS interaction energies increased with increasing amounts of CTA from an average value of $-86 \text{ kcal mol}^{-1}$ for 30 CTA cations to $-54 \text{ kcal mol}^{-1}$ for 90 CTA cations. The increase in the CTA–ZnS interactions could be explained by changes in the arrangement of CTA on the ZnS nanoparticles in dependence on the amount of CTA.

The arrangement of CTA with respect to the ZnS nanoparticle can be characterized by a tilted angle. This is defined as the angle between the tangent plane of a ZnS nanoparticle at the point of the perpendicular projection of nitrogen or the last carbon atom of CTA to the ZnS surface and the CTA chain. In the case of the perpendicular orientation of CTA, the value of the tilted angle is of 90° , while in the case of the parallel arrangement, it is 0° . The tilted angle distribution is shown in Fig. 1 for model 4 and in Figs. S-1–S-3 of the Supplementary material to this paper. Another suitable characteristic of the CTA arrangement is the distribution of nitrogen with respect to the ZnS surface. This is characterized by the distances of the nitrogen of the CTA cations from the ZnS surface and can give us information about a width of the CTA bilayer structure. The distribution is shown in Fig. 2.

In case of 30 CTAs, 14–25 % of CTAs adopted a nearly parallel arrangement with respect to the ZnS surface and more than 60 % of CTAs exhibited an angle lower than 40° with an average of 28° . On the other hand, in case of 90 CTAs, a larger part of the ZnS surface was occupied by CTA cations that tended to adopt an orientation with a higher tilted angle. In this case, less than 10 % of CTAs on average adopted parallel orientation and more than 50 % of CTAs on average exhibited the tilted angle larger than 40° . If the distributions of CTA nitrogen atoms in Fig. 2 are compared, it can see that in case of 30 CTAs, the distance of nitrogen atoms of CTA oriented with their polar headgroups towards to the ZnS surface is about 0.3 nm with a relatively low deviation. In the case of 90 CTAs, the distance and its deviation is higher due to repulsive CTA–CTA inter-

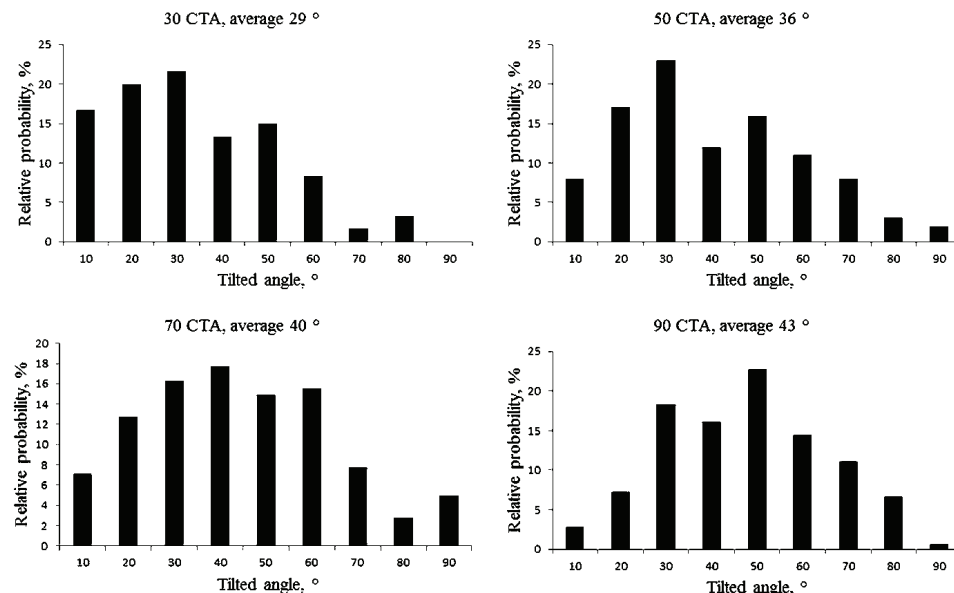


Fig. 1. Angle distribution of the CTAs in model 4 without water.

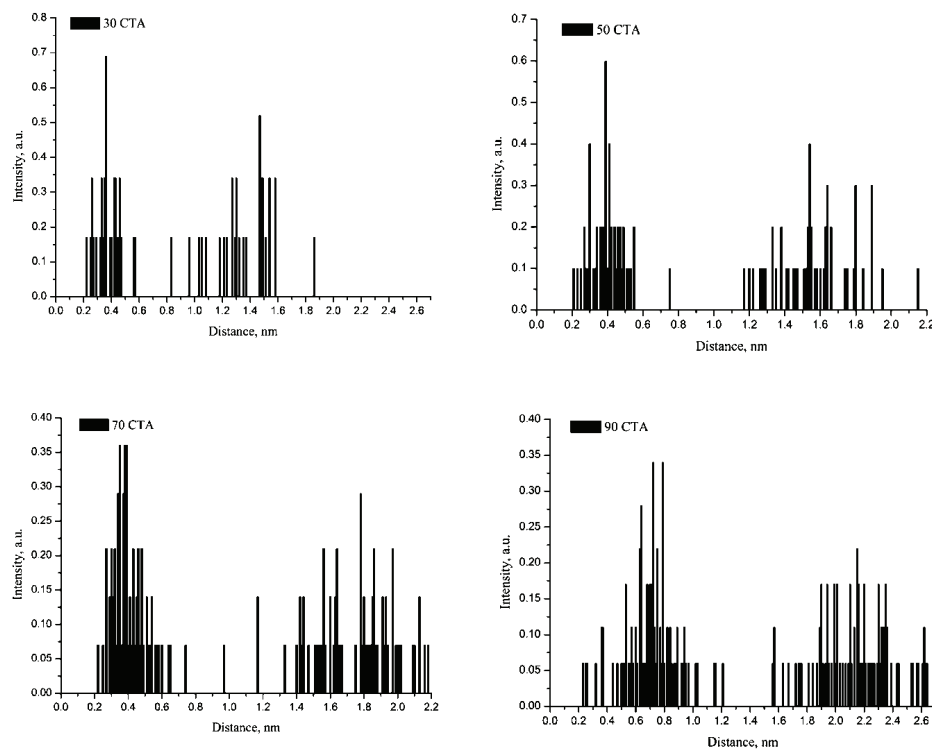


Fig. 2. Distribution of the CTA nitrogen atoms in model 4 without water.

actions leading to a partial expelling of CTA from the ZnS surface, which caused weaker CTA–ZnS interactions.

The mutual interactions between CTA cations depended on the amount of CTA. The van der Waals energy decreased as follows: -5 kcal mol^{-1} on average for 30 CTAs and $-12 \text{ kcal mol}^{-1}$ on average for 90 CTAs. The electrostatic interactions rapidly increasing amount of CTA from $< 1 \text{ kcal mol}^{-1}$ on average for 30 CTAs to 29 kcal mol^{-1} on average for 90 CTAs. The resulting value of mutual CTA interactions was negative in case of 30 CTAs. For 50 CTAs, models 1 and 2 exhibited repulsive CTA–CTA interactions (6 kcal mol^{-1} on average).

Models 3 and 4 exhibited attractive CTA–CTA interactions (-3 kcal mol^{-1} on average) due to the lower electrostatic interactions in comparison to the absolute value of the van der Waals energy. In case of higher amounts of CTA the interactions between CTAs were repulsive: 12 kcal mol^{-1} for 70 CTAs and 17 kcal mol^{-1} for 90 CTAs. Model 4 for 30 CTAs is shown in Fig. 3. Model 4 had the lowest total sublimation energy and, therefore, was the most probable.

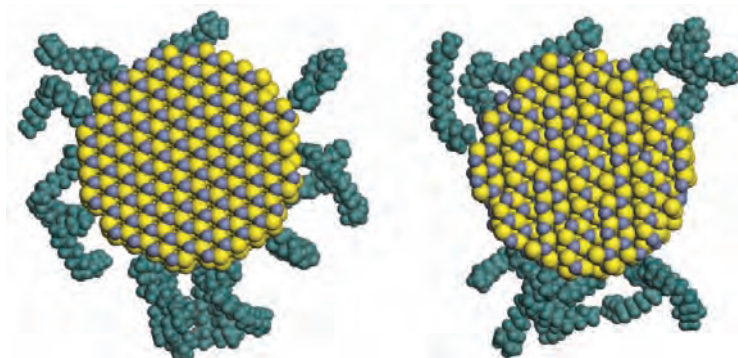


Fig. 3. Cross section of model 4 for 30 CTAs without water. Green chains represent CTA cations.

The interactions between ZnS nanoparticles represented the least energy contribution in the total sublimation energy, *i.e.*, 15 % of the maximum total sublimation energy for model 1. For example, the total sublimation energy in case of 90 CTAs was $-2452 \text{ kcal mol}^{-1}$ and the value of ZnS–ZnS interactions was $-378 \text{ kcal mol}^{-1}$. The interactions between ZnS nanoparticles were calculated only for model 1. For the other models, they were neglected due to the large distance between the nanoparticles. The complete information on the mutual interactions in the systems can be found in Table S-I of the Supplementary material.

Models of ZnS nanoparticles in water environment

In the next modelling calculations, ZnS–CTA particles were simulated in water environment together with bromide anions to be similar to real laboratory

conditions. Total sublimation energies and their components E_{vdw} and E_{elst} were also calculated for different numbers of CTA cations related to each ZnS nanoparticle (30, 50, 70 and 90 CTAs). The non-bonded interactions E representing E_{elst} , E_{vdw} and their sum E_{total} were calculated as follows:

$$E = \frac{E_{(\text{ZnS}-\text{CTA})+\text{Br}+\text{H}_2\text{O}} - E_{\text{H}_2\text{O}} - E_{(\text{ZnS}+\text{H}_2\text{O})}}{n} \quad (1)$$

where $E_{(\text{ZnS}-\text{CTA})+\text{Br}+\text{H}_2\text{O}}$ is the non-bonded interaction energy within all parts of the systems, $E_{\text{H}_2\text{O}}$ represents the interaction energy within the bulk of the water surrounding the ZnS nanoparticles, $E_{(\text{ZnS}+\text{H}_2\text{O})}$ represents the interaction between the ZnS nanoparticles and the surrounding water molecules and n represents the number of CTA cations related to each ZnS nanoparticle. The values of the interactions used in Eq. (1) can be found in Table S-II of the Supplementary material. As in the models without water, the total sublimation energies can be divided into these components: *i*) interactions between CTA cations and water molecules, *ii*) interactions between bromide anions and water molecules, *iii*) interactions between CTA cations and bromide anions and *iv*) interactions between ZnS nanoparticles and water molecules.

First, the interactions between different parts of the system were compared, *i.e.*, the interactions were calculated without mutual repulsive interactions between atoms or molecules in the same part of the system (Br–Br and CTA–CTA interactions). The most significant energy contributions were CTA–H₂O interactions (the interaction energy was calculated only between the bulk of CTA cations and the bulk of water molecules). The average value of these interactions was –440 kcal mol^{–1}. The CTA–Br interactions decreased linearly with increasing amount of CTA, *e.g.*, from –136 kcal mol^{–1} for 30 CTAs to –232 kcal mol^{–1} for 90 CTAs. The Br–H₂O interactions decreased linearly with decreasing amount of bromide, *e.g.*, from –352 kcal mol^{–1} for 30 CTAs to –330 kcal mol^{–1} for 90 CTAs. The interaction energy between one ZnS nanoparticle and water was –19400 kcal mol^{–1} on average. The absolute values of the interactions between CTA cations and ZnS nanoparticles were very low, *i.e.*, 32 kcal mol^{–1} on average. In comparison with the models optimized without water, the absolute values of the CTA–ZnS interactions was about 50 % lower due to strong interactions with water and bromide anions causing a change in the geometry and positions of CTAs with respect to the ZnS nanoparticles. ZnS–ZnS interactions were similar to those calculated for the systems without water and were hundreds of kcal mol^{–1} at the maximum. The absolute value of these interactions was at least two times lower in comparison with total CTA–ZnS interactions (see Table S-I of the Supplementary material). This indicates the ability of CTAs to separate the ZnS–CTA nanoparticles.

Secondly, the average repulsive CTA–CTA and Br–Br interactions increased with increasing amount of CTA cations: 55 kcal mol⁻¹ for 30 CTAs and 109 kcal mol⁻¹ for 90 CTAs. Moreover, the repulsive CTA–CTA interactions in the models with water significantly differed from those without water. As an illustration, the average interaction energy for the systems without water was 7 kcal mol⁻¹ and for the systems in a water environment, it was 33 kcal mol⁻¹. This change was ascribed to CTA–H₂O interactions and CTA–Br interactions, the absolute values of which were much higher in comparison to the CTA–CTA interactions without water. The CTA–H₂O and CTA–Br interactions caused geometry changes of CTA leading to the increase in the CTA–CTA interactions.

The total sublimation energies related to the number of CTAs corresponding to each ZnS nanoparticle are presented in Table II, from which it can see that the total sublimation energies were nearly independent of the number of CTAs. Therefore, CTA cations exhibited a similar probability of being located on the ZnS surface. Due to the lowest interaction energies between different parts in model 1, this model had the lowest total sublimation energy in comparison with the others. Therefore, model 1 was the most probable one and it is presented in Fig. 4 together with models 2, 3 and 4.

TABLE II. Total sublimation energies for the various types of models in a water environment

| No. of CTA cations | $E_{\text{total}} / \text{kcal mol}^{-1}$ | $E_{\text{vdw}} / \text{kcal mol}^{-1}$ | $E_{\text{elst}} / \text{kcal mol}^{-1}$ |
|--------------------|---|---|--|
| Model 1 | | | |
| 30 | -973 | -15 | -958 |
| 50 | -996 | -3 | -993 |
| 70 | -957 | -7 | -950 |
| 90 | -956 | -13 | -943 |
| Model 2 | | | |
| 30 | -845 | -20 | -825 |
| 50 | -895 | -3 | -892 |
| 70 | -864 | -1 | -863 |
| 90 | -906 | 7 | -913 |
| Model 3 | | | |
| 30 | -935 | -4 | -931 |
| 50 | -916 | -11 | -905 |
| 70 | -892 | -12 | -880 |
| 90 | -861 | -22 | -839 |
| Model 4 | | | |
| 30 | -894 | -5 | -889 |
| 50 | -845 | -10 | -835 |
| 70 | -872 | -10 | -862 |
| 90 | -931 | -17 | -914 |

The coverage of the surface depended on the CTA concentration and it could be estimated by calculating the surface area of the ZnS nanoparticle occupied by

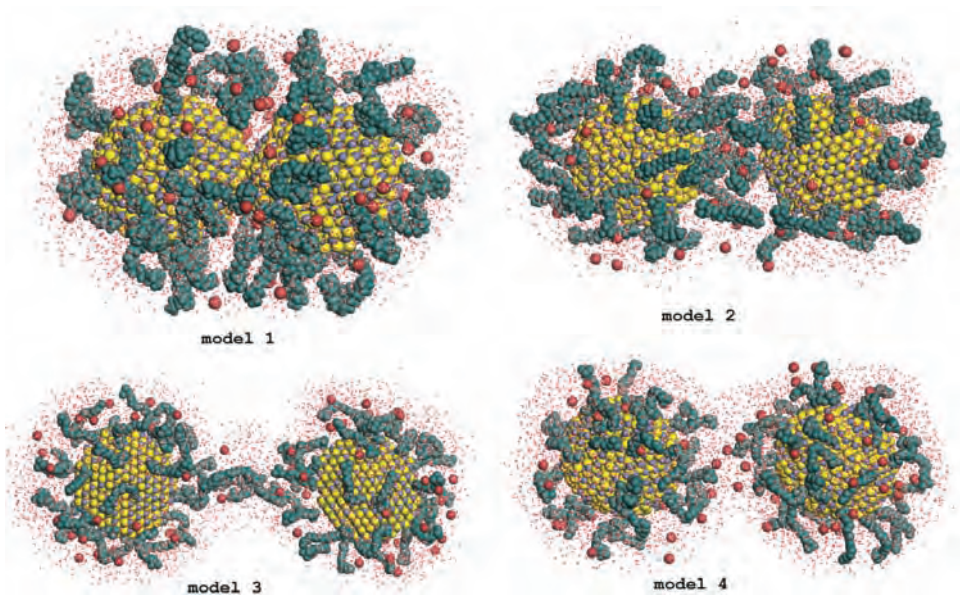


Fig. 4. ZnS nanoparticles of models 1–4 with water surrounded by 30 CTA cations and compensating bromide anions. The green chains represent CTA cations and the brown balls represent bromide anions.

headgroups and by the ends of CTA chains using van der Waals radii. One polar headgroup occupies 0.27 nm^2 and 0.04 nm^2 is occupied by one end of CTA. The coverage of the ZnS nanoparticle surface with a radius of 2 nm is of 9, 15, 22 and 28 % in case of 30, 50, 70 and 90 CTAs, respectively. If the fact that the orientation of CTA is tilted with respect to the ZnS nanoparticle is taken into account, a higher coverage of the surface could be expected. Nevertheless, the ZnS nanoparticles are not “hermetically” isolated by CTA from the surrounding water environment (see Fig. S-4 in the Supplementary material) and the CTA cations tend to form sparse covers around the nanoparticles. This indicates that these nanoparticles should grow in time, which was verified by a study of the growth kinetics. A final radius of 2.46 nm after 24 h was determined and no coagulation was observed. In addition, the recently evidenced photocatalytic activity of ZnS–CTA nanoparticles in the decomposition of phenol¹⁸ confirms that various chemical compounds can move to the surface of such nanoparticles to react with photo-generated hydroxyl radicals.

As for the models without water, the CTA arrangement on the ZnS surface can be described by the angle distribution, as shown in Fig. 5 for model 1. The angle distributions for models 2, 3 and 4 are given in the Supplementary material (Figs. S-5–S-7). In case of the lower concentrations of CTA, the average angle values in the models with water were about 10 higher than those without water,

while at higher CTA concentrations, the average angle values were comparable to those without water. The average angle values ranged in the interval of 35–49°. In case of model 1, the angle values range in the interval of 40–45°.

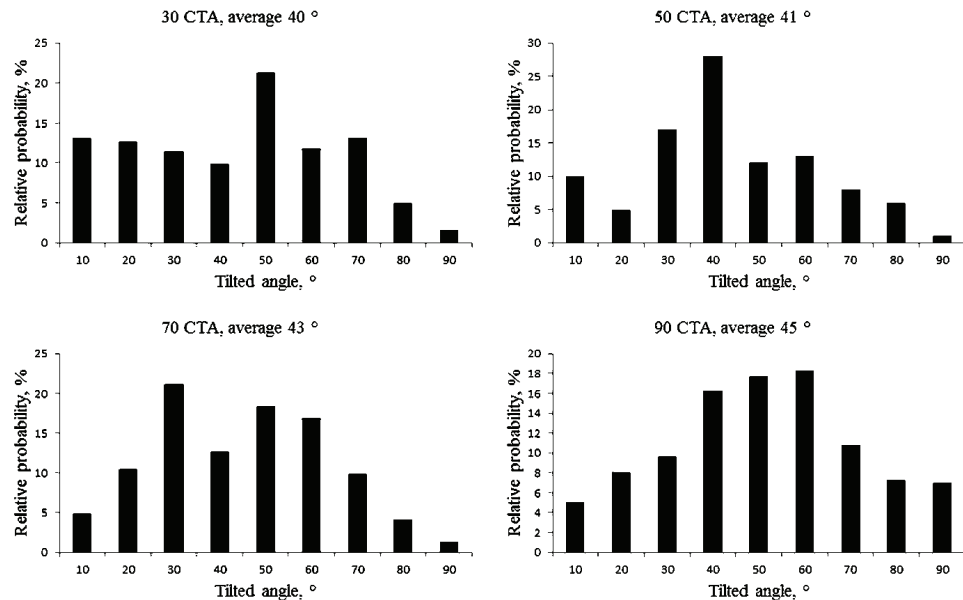


Fig. 5. Angle distribution of CTAs in model 1 with water.

The TEM micrograph presented in Fig. 6 shows the agglomeration of ZnS–CTA nanoparticles into flocs (flakes of precipitate that come out of solution during flocculation) of different sizes. The size histogram is included in Fig. 6 as

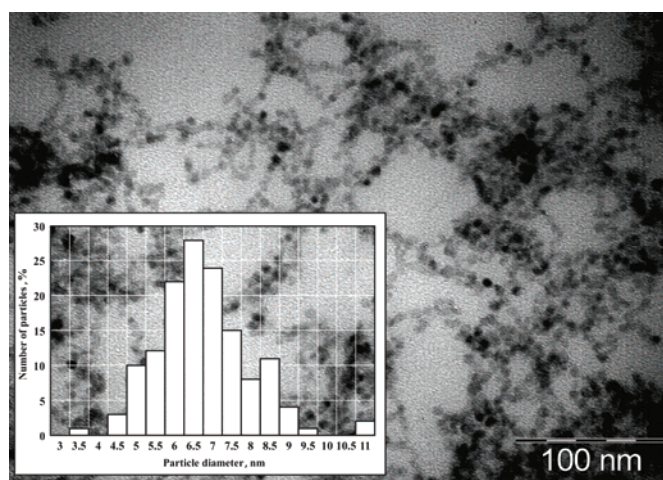


Fig. 6. TEM micrograph of ZnS–CTA dispersion.

well. The mean radius was determined to be about 3.25 nm. This value covers the radii of ZnS nanoparticles and the thickness of the CTA cover around it. The radii of single ZnS nanoparticles increased from 2.07 to 2.39 nm within a time interval of 0.05–3 h at room temperature. At longer times up to 24 h the radii increased up to 2.46 nm. These radii were calculated based on band-gap energies estimated from UV spectra of ZnS colloid dispersions as described, *e.g.*, in our earlier papers.^{4,6} The TEM micrograph was obtained during the early stage of the ZnS nanoparticles growth, that is, at 3 min when the calculated ZnS nanoparticles radius was about 2 nm. Sizes of these flocs in a range of 9–122 nm with a modus of 16 nm were found by the dynamic light scattering method.⁵

The results of TEM compared with models 1–4 showed that ZnS nanoparticles tended to adopt the mutual arrangement close to that presented in model 1. The flocs with the size of 9 nm likely correspond to the case when they are consisted of two ZnS nanoparticles touching each other as it is shown in Figure 4. Total sublimation energy values of model 1 were about 9 % lower on average in comparison with other types of models. It indicates that one can expect the occurrence of these models with lower probability. Figure 6 shows that some ZnS nanoparticles are isolated by CTA or joined together by CTA chains (see Fig. 4). The histogram of diameters of nanoparticles (Fig. 6) represents the sum of ZnS nanoparticle diameter and the thickness of the bilayer that can be characterized by distances of outer nitrogen atoms of CTA and ZnS nanoparticle surface. All types of models exhibited similar distributions of nitrogen atoms and they are demonstrated for model 1. The results of modelling showed a weak dependence of total sublimation energy on the number of CTAs surrounding ZnS nanoparticles and we can suppose that CTAs of all studied concentrations have similar probability to be located on ZnS nanoparticle surface.

Figure 7 shows a combination of distributions of nitrogen atoms for all studied concentrations in model 1 fitted by a polynomial of 9th order to obtain the best fit. We can observe three maxima. The first maximum at the distance of 0.3 nm corresponds to the nitrogen atoms of CTAs with their polar headgroups oriented towards the surface of the ZnS nanoparticle. The distance between the nitrogen atom and the hydrogen atom of the polar headgroup is 0.15 nm and, if one take into account the van der Waals radius of hydrogen atom, *i.e.*, 0.06 nm, it could be stated that the polar headgroups nearly touch the surface of the ZnS nanoparticle. The other maxima at 1.5 and about 2.2 nm represent the positions of outer CTA nitrogen atoms. If a ZnS nanoparticle radius of 2 nm is considered and the length of CTA cation represented by the maximum at 1.5 nm, a total diameter of 7 nm is obtained, which is close to the maximum at 6.5 nm obtained from TEM measurements. The maximum at the distance of 2.2 nm (8.4 nm in diameter) is in agreement with the measured distance of 8.5 nm. It shows good agreement between the experimental and calculated results.

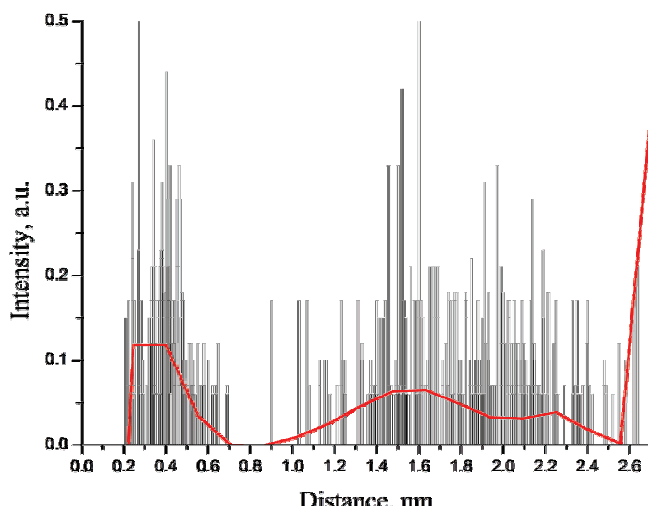


Fig. 7. Distribution of CTA nitrogen atoms in model 1 with water.

CONCLUSION

ZnS nanoparticles stabilized by CTAB were modelled in the Materials Studio environment. The nanoparticle geometry was optimised in the Universal force field and charges of ZnS nanoparticles were calculated by the QEq method. The partial charges of water molecules and CTA cations were assigned by the Compass force field. ZnS nanoparticles with radii of 2.0 nm surrounded with various amounts of CTA cations were modelled without water and in a water environment. Four models with different distances between the ZnS nanoparticles and the arrangement of the CTA cations were built and characterized by calculated sublimation energies.

Based on the molecular modelling results without water, it could be concluded that the most favourable model consisted of two ZnS nanoparticles at a distance of 8–9 nm separated without immersing CTAs. In a water environment, the energies of the ZnS–CTA interactions were significantly higher than in vacuum. The most favourable model was composed of two ZnS nanoparticles that nearly touched each other. The CTA cations acted as a sparse cover around the ZnS nanoparticles and exhibited a tilted orientation with respect to ZnS nanoparticle surface with tilted angle values ranging from 26 to 43° in the models without water and from 35 to 49° in the models with water. Size histogram of ZnS–CTA particles measured by TEM was compared with the models using the distribution of outer nitrogen atoms and good agreement between the experiment and calculated results was obtained.

SUPPLEMENTARY MATERIAL

Figures S-1–S-7 and Tables S-I and S-II are available electronically from <http://www.shd.org.rs/JSCS/> or from the corresponding author on request.

Acknowledgements. This work was supported by the Czech Science Foundation (P107/11/1918), by the Ministry of Education, Youth and Sports of the Czech Republic in the “National Feasibility Program I” (project LO1208 “TEWEP”), by the Regional Materials Science and Technology Centre (CZ.1.05/2.1.00/01.0040) in Ostrava and by VŠB-Technical University of Ostrava (SP 2014/55), Czech Republic.

ИЗВОД

МОЛЕКУЛСКО МОДЕЛОВАЊЕ ПОЛОЖАЈА ЦИНК-СУЛФИДНИХ НАНОЧЕСТИЦА
СТАБИЛИСАНИХ ЦЕТИЛТРИМЕТИЛАМОНИЈУМ-БРОМИДОМ

PETR KOVÁŘ¹, PETR PRAUS^{2,3}, MIROSLAV POSPÍŠIL¹ и RICHARD DVORSKÝ⁴

¹Charles University in Prague, Faculty of Mathematics and Physics, Ke Karlovu 3, 12116 Prague 2, Czech Republic, ²Regional Materials Science and Technology Centre, VŠB-Technical University of Ostrava, 17. Listopadu 15, 708 33 Ostrava-Poruba, Czech Republic, ³Department of Chemistry, VŠB-Technical University of Ostrava, 17. Listopadu 15, 708 33 Ostrava-Poruba, Czech Republic и ⁴Institute of Physics, VŠB-Technical University of Ostrava, 17. Listopadu 15, 708 33 Ostrava-Poruba, Czech Republic

Положај ZnS наночестица стабилисаних цетилтритемиламонијум-бромидом (СТАВ) моделована је у *Materials Studio* програмском окружењу. Постављена су четири модела са различитим растојањима између ZnS наночестица и различитом количином СТАВ у неводеној и воденој средини и окарактерисана помоћу израчунатих енергија сублимације. Резултати у неводеној средини без СТАВ су показали да се најповољнији модел састоји од две ZnS наночестице на растојању од 8 до 9 nm. С друге стране, у воденој средини најповољнији модел предвиђа да се наночестице готово додирују. СТАВ показује тенденцију смештања са ретким паковањем на површину наночестица. Расподела ZnS–СТА већица по величини која је добијена трансмисионом електронском микроскопијом добро се слагала са резултатима добијеним молекулском моделовањем.

(Примљено 15. новембра 2013, ревидирано 28. фебруара, прихваћено 10. маја 2014)

REFERENCES

1. D. Schroder, *Semiconductor Material and Device Characterization*, Wiley, New York, 2006
2. Z. Wang, N. Herron, *J. Phys. Chem.* **95** (1991) 525
3. L. E. Brus, *J. Chem. Phys.* **80** (1984) 4403
4. P. Praus, R. Dvorský, P. Horíková, M. Pospíšil, P. Kovář, *J. Colloid Interf. Sci.* **377** (2012) 58
5. P. Praus, R. Dvorský, P. Kovář, J. Trojková, *Acta Chim. Slov.* **59** (2012) 784
6. O. Kozák, P. Praus, K. Kočí, M. Klementová, *J. Colloid Interf. Sci.* **352** (2010) 244
7. S. Hamad, S. M. Woodley, C. R. Catlow, *Mol. Simul.* **35** (2009) 1015
8. H. Zhang, B. Chen, Y. Ren, G. A. Waychunas, J. F. Banfield, *Phys. Rev., B* **81** (2010) 125444.
9. F. Huang, B. Gilbert, H. Zhang, J. F. Banfield, *Phys. Rev. Lett.* **92** (2004) 155501-1
10. B. Gilbert, H. Zhang, F. Huang, J. F. Banfield, *J. Chem. Phys.* **120** (2004) 11785
11. C. J. Yang, X. Chen, Z. M. Sui, L. Y. Wang, *Colloids Surfaces, A* **274** (2006) 219
12. J. Yue, X. C. Jiang, Q. H. Zeng, A. B. Yu, *Solid State Sci.* **123** (2011) 1152

13. J. W. Anthony, R. A. Bideaux, K. W. Bladh, M. C. Nichols, *Handbook of Mineralogy*. Mineralogical Society of America, Chantilly, USA, <http://www.handbookofmineralogy.org> (accessed on 25th October 2013)
14. *Materials Studio Modeling Environment*, Release 4.3 Documentation, Accelrys Software Inc., San Diego, CA, 2003
15. A. K. Rappe, C. J. Casewit, K. S. Colwell, W. A. Goddard, W. M. Skiff, *J. Am. Chem. Soc.* **114** (1992) 10024
16. A. K. Rappe, W. A. Goddard, *J. Phys. Chem.* **95** (1991) 3358
17. H. Sun, D. Rigby, *Spectrochim. Acta, A* **53** (1997) 1301
18. P. Praus, J. Matys, O. Kozák, *J. Braz. Chem. Soc.* **23** (2012) 1900.